Density-of-States Based Numerical and Analytical Models for Solution-Processed Polymer TFTs

Jaeman Jang, Jaewook Lee, Hyeongjung Kim, Sung-Jin Choi, Dong Myong Kim, and Dae Hwan Kim[a)]

School of Electrical Engineering, Kookmin University, 861-1 Jeongneung-dong, Seongbuk-gu, Seoul 136-702, Korea
[a)]*E-mail: drlife@kookmin.ac.kr*

Abstract

In this work, we propose the subgap density-of-states (DOS) based design platform for solution-processed polymer-based thin-film-transistors (PTFTs). For the model simulation, numerical and analytical I-V models were established from experimentally extracted DOS parameters, and verified by comparing the simulation result with the measured characteristics of solution-processed PTFTs.
Keywords: solution process; organic; polymer; thin-film transistors; density-of-states; analytical model; circuit simulation.

1. Introduction

A great deal of attention has been paid recently to organic electronics, driven by their potential applications throughout from flexible displays [1], large area sensors [2], and radio frequency identification tags [3] to flexible processors [4] and customized programmable logics [5]. In these approaches, polymer-based thin-film-transistors (PTFTs) are the fundamental building blocks with their advantages of low-cost, low-temperature process, and compatibility with the solution process such as spin-coating, ink-jet printing, and gravure printing. However, the circuit simulation method for the solution processed PTFTs has been rarely researched yet while a number of OTFTs with high field-effect mobility higher than 0.1 $cm^2/V{\cdot}s$ have been reported using ink-jet printing [6], [7]. As their potential application becomes more diverse and challenging, the demand for device-circuit co-design, which should be described preferably only with the process/material-controlled and experimentally extracted parameters rather than fitting parameters, becomes indispensable in the solution-processed organic integrated circuits. In this work, we developed the numerical and analytical PTFT models based on the process-controlled parameters including subgap density-of-states (DOS:$g(E)$).

2. Device fabrication and structure

The polymer-based organic semiconductor was dissolved in tetrahydronaphthalene (THN) at a concentration of 0.2 wt%, and then ink-jet printed via Dimatix printer. The fabricated PTFTs with a coplanar structure had the channel width (W)=120 μm, the gate-to-source/drain (S/D) overlap length (L_{OV})=10 μm, gate insulator thickness (T_{OX})=300 nm, and thickness of polymer film ($T_{Polymer}$)=50 nm (confirmed by FIB-SEM), respectively. Fig. 1(a) shows an array of semitransparent polymer transistors printed on a glass substrate. Fig. 1(b) shows a schematic cross-sectional view of the PTFT with a coplanar structure.

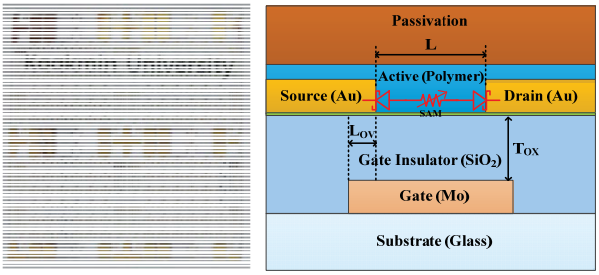

(a) (b)

Fig. 1. (a) A photograph of PTFTs and circuit integrated on a glass wafer. (b) A schematic illustration of the integrated PTFT with the bottom gate and bottom source/drain contact structure (with a coupled-Schottky diode model).

3. Density-of-states Based numerical and analytical models

Fig. 2 shows a schematic illustration of $g(E)$ in polymer thin-film materials. The $g(E)$ is comprised of the donor-like states ($g_D(E)$), shallow acceptor-

like states ($g_{SA}(E)$), and interface trap ($D_{it}(E)$). The $g(E)$ modeled by a superposition of exponential tail and deep states and Gaussian shallow states as follows:

$$g(E) = g_{DD}(E) + g_{TD}(E) + g_{SA}(E)$$
$$= N_{TD} \times \exp\left(\frac{E_V - E}{kT_{TD}}\right) + N_{DD} \times \exp\left(\frac{E_V - E}{kT_{DD}}\right) + N_{SA} \times \exp\left[-\left(\frac{E_{SA} - E}{kT_{SA}}\right)^2\right] \quad (1)$$

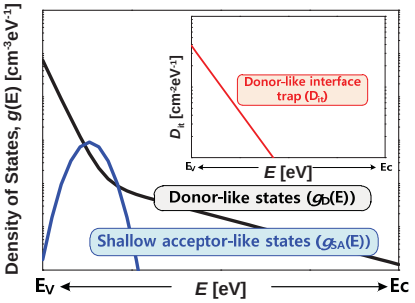

Fig. 2. A schematic illustration of $g(E)$ of the polymer material. It consists of donor-like DOS; $g_D(E)$ (it is extracted from the *MFCV* spectroscopy) and the shallow acceptor-like DOS; $g_{SA}(E)$ (it is extracted from a fitting with measured data by numerical model simulation.). The inset shows a schematic illustration of the interface trap density, $D_{it}(E)$.

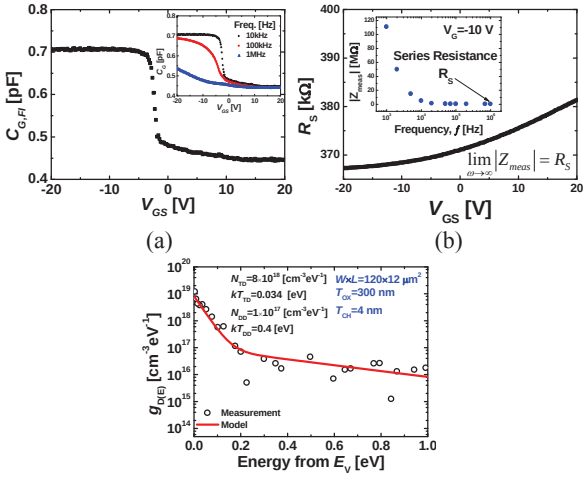

Fig. 3. Extraction of $g_D(E)$ using the *MFCV* spectroscopy (a) The calculated $C_{G,FI}$ from f-dependent C_G-V_G characteristics is shown as an inset. (b) Extracted V_{GS}-dependent R_S obtained from the high frequency $|Z_{meas}|$ under a fixed V_{GS} as shown in the inset. (c) Extracted $g_D(E)$.

The extraction procedure of $g_D(E)$ by the Multi-frequency C-V (*MFCV*) spectroscopy is shown in Fig. 3. This method has been published in the [8]. Fig. 4 shows the calculation flow about numerical and analytical current-voltage (*I-V*) models. The models start with $g_D(E)$ obtained by the *MFCV* spectroscopy. As shown in Fig. 4 (a) Numerical models are based on physics-based parameters not fitting parameters. The $g_D(E)$ was experimentally extracted, while $g_{SA}(E)$ and $D_{it}(E)$ were extracted from the numerical iteration. The proposed numerical model is expected to be a useful platform for systematic design of PTFTs via the material/process optimization.

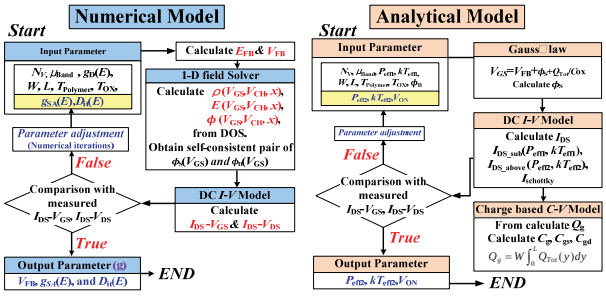

Fig. 4. The calculation flow for the numerical & analytical *I-V* models with same parameters ($g_D(E)$, μ_{BAND}, N_V). (a) Numerical model flow: TFT's structural parameters are given as W, L, $T_{Polymer}$, T_{OX}. The $g_D(E)$ experimentally extracted then the other parameters (N_V, μ_{BAND}) are determined. The V_{FB} & E_{FB} are calculated with the potential obtained from the 1-D field solver. (b) Analytical model flow: The Input parameters (P_{effl}=N_{TD}, kT_{effl}=kT_{TD}, W, L, T_{OX}, Schottky barrier(ϕ_B)) are fixed by known or extracted value. Through the Gauss' law, calculate the surface potential and then calculate I_{DS}.

On the other hand, as shown in Fig. 4 (b) the analytical model is based on the effective carrier density combined with a coupled-Schottky diode model (in Fig. 1 (b)) for the non-linearity and the Poole-Frenkel mobility model for the lateral field-dependent carrier transport. We expect that the proposed analytical model can be employed for a fast and efficient circuit design. We obtain an analytical model for drain current caused by the drift of holes in the channel as

$$I_{DS}\left(N_{effi}, kT_{effi}\right) = \frac{W}{L}\mu_{Band} e^{\beta\sqrt{|V_{DS}|/L}} \frac{A^* N_V}{2P_{effi} kT_{effi} C^*} \left(\frac{C_{OX}}{\sqrt{2\varepsilon_P P_{effi} kT_{effi}}}\right)^{-2C^* kT_{effi}}$$
$$\times \left[\frac{1}{\left(-2C^* kT_{effi}+1\right)}\left\{\left(V_{GS}-V_{FB}-\phi_{SS}\right)^{-2C^* kT_{effi}+1} - \left(V_{GS}-V_{FB}-\phi_{SD}\right)^{-2C^* kT_{effi}+1}\right\}\right.$$
$$\left. -\frac{1}{-qC^*}\left\{\left(V_{GS}-V_{FB}-\phi_{SS}\right)^{-2C^* kT_{effi}} - \left(V_{GS}-V_{FB}-\phi_{SD}\right)^{-2C^* kT_{effi}}\right\}\right] \quad (2)$$

And from the Schottky diode current equation is

$$I_{Schottky} = AA^{**}T^2 e^{-q\phi_B/\eta kT}\left(e^{qV_{DS}/\eta kT} - 1\right) \quad (3)$$

Finally, the total drain current over the sub- and above-V_T regions for the PTFT modeled as a series connection of the Schottky diodes at S/D contacts with the V_{GS}-dependent channel resistance can be described by

$$\frac{1}{I_{DS}} = \frac{1}{I_{DS\_sub}(P_{eff1}, kT_{eff1})} + \frac{1}{I_{DS\_above}(P_{eff2}, kT_{eff2})} + \frac{1}{I_{Schottky}} \quad (4).$$

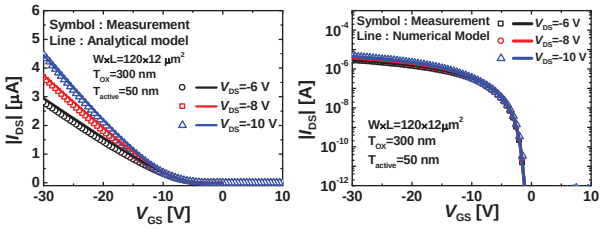

(a) (b)

Fig. 5. Calculated I_{DS}-V_{GS} characteristics from numerical model (line) (a) linear scale and (b) semi-log scale (V_{DS}=-6 ~-10 V) compared with the measured ones (symbol) for a PTFT.

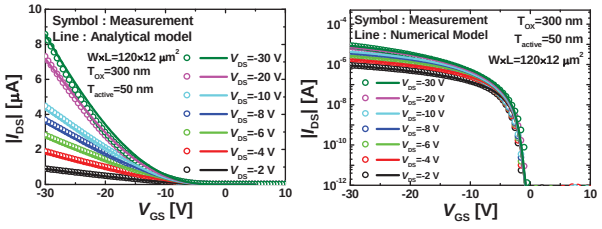

(a) (b)

Fig. 6. Calculated I_{DS}-V_{GS} characteristics from the analytical model (line) (a) linear scale and (b) semi-log scale (V_{DS}=-2~-30 V) compared with the measured ones (symbol) for a PTFT.

Fig. 5 and Fig. 6 shows verification of models by comparing the measured I_{DS}-V_{GS} characteristics with calculated results over a wide range of the gate/drain bias. Model parameters are summarized in Table. I. We note that model parameters of the two models are interconnected each other(N_{TD}=P_{eff1}, kT_{TD}=kT_{eff2}).

Table I. Model parameters based on physical properties. The parameters, such as g_D(E), μ_{BAND}, Nv, N_{TD}= P_{eff1}, and kT_{TD}=kT_{eff1} are commonly used for the two models.

Common	μ_{BAND}	N_V	N_{TD}	kT_{TD}
	0.146	2.5×10^{19}	8×10^{18}	0.034
Numerical Model	N_{DD}	kT_{DD}	N_{itD}	kT_{itD}
	1×10^{17}	0.4	1.2×10^{12}	0.2
	N_{SA}	kT_{SA}	E_{SA}	
	1×10^{17}	0.1	0.25	
Analytical Model	V_{ON}	ϕ_B	P_{eff2}	kT_{eff2}
	-1.5	0.45	2.6×10^{19}	0.0283

The calculated results agree well with the measured ones over wide range of V_{GS} and V_{DS}. We suggested that the detailed nonlinearity of PTFTs was successfully reproduced with our improved model.

4. Conclusion

We reported analytical and numerical *I-V* models for solution-processed PTFTs based on the process-controlled parameters including DOS. Our approach also made it possible to co-design with the definite relationship between the process/material and the device characteristics because most of all parameters can be controlled by either the process or the material.

5. Acknowledgements

This work was supported by the National Research Foundation of Korea (NRF) grant funded by the Ministry of Education, Science and Technology (MEST) (Grant no. 2012-0000147). The devices were supported by Samsung Advanced Institute of Technology (SAIT).

References

[1] M. Mizukami *et al.*, "Flexible AM OLED panel driven by bottom-contact OTFTs", *IEEE Electron Device Lett.*, vol. 27, pp. 249-251, Apr. 2006.

[2] M. Zirkl *et al.*, "Low-Voltage Organic Thin-Film Transistors with High-k Nanocomposite Gate Dielectrics for Flexible Electronics and Optothermal Sensors", *Adv. Mater.*, vol. 19, pp. 2241-2245, July 2007.

[3] M. Jung *et al.*, "All-Printed and Roll-to-Roll-Printable 13.56-MHz-Operated 1-bit RF Tag on Plastic Foils", *IEEE Trans. Electron Device*, vol. 57, pp. 571-580, Mar. 2010.

[4] K. Myny *et al.*, "An 8b organic Microprocessor on plastic Foil," in *ISSCC Dig. of Tech. Papers*, p. 322, 2011.

[5] K. Ishida *et al.*, "User Customizable Logic Paper (UCLP) With Sea-Of Transmission-Gates (SOTG) of 2-V Organic CMOS and Ink-Jet Printed Interconnects", *Solid-State Circuits, IEEE Journal of*, vol. 46, pp. 285-292, Jan. 2011.

[6] S. H. Lee *et al.*, "High-performance thin-film transistor with 6,13-bis(triisopropylsilylethynyl) pentacene by inkjet printing", *Org. Electron.*, vol. 9, pp. 721-726, Oct. 2008.

[7] G. L. Whiting, and A. C. Arias, "Chemically modified ink-jet printed silver electrodes for organic field-effect transistors", *Appl.Phys. Lett.*, vol. 95, p. 253302, Dec. 2009.

[8] J. Jang *et al.*, "Extraction of the sub-bandgap density-of-states in polymer thin-film transistors with the multi-frequency capacitance-voltage spectroscopy", *Appl. Phys. Lett.*, vol. 100, p. 133506, Mar. 2012.